
Article:
Wang, Q., Zhang, Y. orcid.org/0000-0002-9736-5043 and Zhao, C. (2018) Experimental Investigation of Co-flow Effect on Ignition Process of a Methane Jet Diffusion Flame. Experimental Thermal and Fluid Science, 91. pp. 184-196. ISSN 0894-1777

https://doi.org/10.1016/j.expthermflusci.2017.10.016

Experimental Investigation of Coflow Effect on the Ignition Process of a Methane Jet Diffusion Flame

Qian Wang[a](✉), Yang Zhang [b], C.Y. Zhao [a]

[a] School of Mechanical Engineering, Shanghai Jiao Tong University, Shanghai, 200240, China

[b] Department of Mechanical Engineering, the University of Sheffield, Sheffield, S1 3JD, UK

Email: qianwang@sjtu.edu.cn

Phone: +86(21)34204541
Fax: +86(21)34206092

Abstract

The coflow air effect on the ignition process of a methane jet diffusion flame has been investigated using high speed colour/schlieren imaging and image processing techniques experimentally. The methane flow rate is kept at constant (Re=55.4), while the coflow air flow rate changes (Re from 171 to 5985), creating a wide range of the air/fuel velocity ratios varying from 0.36 to 12.5. Special digital image processing techniques are applied to visualise the weak blue flame and weak yellow flame, which is often difficult to view in the presence of the bright orange diffusion flame, during ignition process. The processed images have shown clearly that a sooty diffusion flame is initially formed inside a blue flame pocket at low air velocities. When the coflow air flow rate exceeds 75 l/min, only blue flame can be observed. The equivalence ratio of blue flame has been evaluated based on colour characteristics, which is close to 1 during the ignition process for all the cases. Moreover, the fuel flow, flame and hot gas interactions with the cold air flow are investigated by visualising the schlieren images. It is found that a hot gas bulge is formed due to the excessive fuel exiting before ignition and a hot laminar central jet is formed with the help of coflow effect. The hot gas bulge tip and bottom moving velocities are found to increase with the coflow air flow rates. Besides flow visualisation based on high-speed schlieren imaging sequences, the velocity fields during ignition process have been evaluated quantitatively using optical flow method.

Keywords: Ignition; Diffusion methane flame; Coflow; High speed imaging; Schlieren.

1. Introduction

Laminar gas jet diffusion flames have been intensively studied in combustion science [1-6]. Diffusion flames are widely used in industrial systems for safety consideration, since the oxidizer and fuel can be stored separately. In order to improve the stability of diffusion flames, adding coflow is often

considered to be an effective and easy implementation method. Characteristics of diffusion flames in laminar jets have been investigated extensively to understand the stabilization mechanism both for lifted and attached flames.The lift-off characteristics in coflow jets with highly diluted propane were studied experimentally [7]. The gravity effects on the oscillation mechanisms of a lifted flame have been tackled under coflow conditions in [8]. A combined computational and experimental investigation that examines the relationship of soot and NO formation in coflow ethylene air diffusion flames is presented in [9]. The coflow effect on the interaction between the visible flame and outside vortices of the non-lifted methane diffusion flames have been studied systematically through experimental visualisation methods [10]. It is found that coflow air can help to push the initiation point of toroidal vortex to exceed the flame tip; the flame oscillation induced by the vortex is then suppressed. However, the aforementioned research mainly focused on the well-established flame dynamics; the ignition process of diffusion flame with coflow is rarely studied.

The ignition of a flammable mixture is a fundamental problem in the field of combustion science, which involves complex chemical reactions and flow variations. Many technological applications requires detailed investigation on the combustion transition from a non-reacting (forced ignition) or a slow reacting state (auto ignition) to a fully burning state; for example, the relighting of an aviation gas turbine, the spark-ignition engine and diesel engine, etc. The initiation of turbulent non-premixed flames through auto ignition and spark ignition has been reviewed by Mastorakos [11]. Phuoc et al. [12] investigated the laser spark ignition of a jet diffusion flame experimentally. It is reported that the success of ignition depends on whether the spark initiated reacting gas could undergo a transition from hot plasma to a propagating flame or not. The simulation work by Richardson ES and Mastorakos E. [13] indicates that the ignition can be prohibited by excessive strain rates in a non-premixed flame. The ignition and flame propagation of a methane-air triple flame in a partially premixed jet is investigated experimentally and numerically by Qin et. al.[14]. It is found that during the flame propagation process, the curvature-induced stretch dominates over the hydrodynamic stretch and the flame speed decreases with the increase of stretch rate. Zhang and Bray [15] reported that different

flame patterns can be formed under identical flow conditions only by varying the ignition place for a methane impinging flame. The ignition process of methane and propane diffusion impinging flame was further investigated by Wang and Huang [16, 17] through high speed colour/schlieren and image processing techniques. It is found that the ignition process is sensitive to plate-to-nozzle height, fuel flow rate, ignition position and fuel type. Most of the aforementioned ignition studies focus on minimum ignition energy, strain rates effect and ignition probability, with most of which only considering premixed flames. For non-premixed flames, the forced ignition process is more complicated, as confirmed by both simulations and experiments. The experimental ignition data under particular flow conditions may help to gain more physical insights into the understanding of non-premixed ignition process. In this study, the coflow air effect on the ignition process of methane diffusion flame is explored experimentally, which has not been reported to the best knowledge of the authors.

A modern high-speed colour camera is not only able to visualise the behaviours of time-dependent flame structure evolution but also provides dynamic information on the flame colour change. For hydrocarbon flames, the visible emanating energy can be attributed to the spectra of electronically excited combustion radicals CH* (430 nm), C_2* (C_2* Swan system, dominant emissive band head at 473.71 nm and 516.52 nm), CN* (350-380 nm) and the continuous spectrum from solid carbon/soot [18]. The intensity of the energy released by these spectra is related to a number of factors such as burning condition, fuel composition and fuel-to-oxidizer ratio, which would consequently affect the colour perceived from a given flame. Thus, the colour of a flame can be used to provide information on its general spectrometric composition. Modern digital high-speed colour cameras, unlike its more commonly employed monochromatic counterpart, encodes the captured visible radiation into three discrete signal ranges with sensitively peaking in the R, G and B portion of the visible electromagnetic spectrum. In this form, digital colour cameras can be considered as a device that offers limited multi-spectral discrimination in addition to its designed spatial functionality. The blue and green emissions (in the RGB colour space) were found to model well the CH* and C_2* chemiluminescence intensities,

respectively. Based on this, a Digital Flame Colour Discrimination (DFCD) combustion quantification scheme has been established by Huang and Zhang [19]. In the DFCD method, the appropriate use of colour signals identified from the different flame radiation induction regime is able to provide useful correlations such as indicating the trends of spectroscopic-derived CH* and C_2* emission distributions over range of equivalence ratios [20], and the local fuel/air mixing [17]. It also has demonstrated useful application in identifying the concurrent existence of weak chemiluminescence induced kernel volumes that along with the dominant soot continuum-radiation during the ignition of non-premixed hydrocarbon flames in both the laboratory Bunsen burner [20] and the optical combustion chamber ignition sequences [21]. In this study, the DFCD method has been applied to reveal otherwise difficult to visualise flame initiation process, while the hot gas evolution outside the visible flame has been investigated via schlieren imaging. Quantitative velocity fields have been estimated based on the schlieren image sequences using optical flow method. The coflow effects on the cold flow pattern, mixture fraction distribution, flame propagation, flow speed, as well as the soot formation have been investigated and analysed comprehensively. The results have provided improved physical insights into the nature of ignition process and should provide useful validation data for modeling studies.

2. Experimental methods

The schematic setup of the experimental system is shown in Fig. 1. In the experiments, methane was used as fuel. The air and fuel was controlled by mass flow controllers. The fuel jet was surrounded by a coaxial air jet. The fuel was injected through a central nozzle of 4.57 mm in diameter. The coflow air nozzle has a diameter of 37.8 mm. The air was straightened by a fine meshed honeycomb inside the air nozzle. The detail structure of the burner can be referred to [10]. A Z-type schlieren imaging system was used to investigate the flow dynamics and structures. The schlieren system consists of a LED lamp as the light source and two parabolic mirrors with 0.3048 m (12 in.) in diameter and 3.048 m (10 feet) in focal length. The images were recorded by a high speed camera (Photron FASTCAM SA4) with a resolution of 1024 by 1024 pixels. Table 1 shows the test conditions of the experiments.

The fuel flow rate was fixed at 0.182 l/min, while the coflow air flow rate was ranging from 5 l/min to 175 l/min. The calculation of Reynolds number of fuel and air is based on the fuel nozzle diameter and coflow nozzle diameter respectively. The velocity ratio between air and fuel varies in a wide range from 0.36 to 12.5. Electric spark from a Kawasaki ignition-coil (TEC-KP02) was generated between a pair of steel electrodes with sharpened edges to reduce the heat loss. The electric charge to the coil was delivered from a sealed lead acid battery (12 volt, 1.2 Ah) to produce a consistent spark voltage of approximately 30 kV. The ignition electrodes were placed at a distance of 14 mm downstream of the burner nozzle exit with a spark gap of 9 mm.

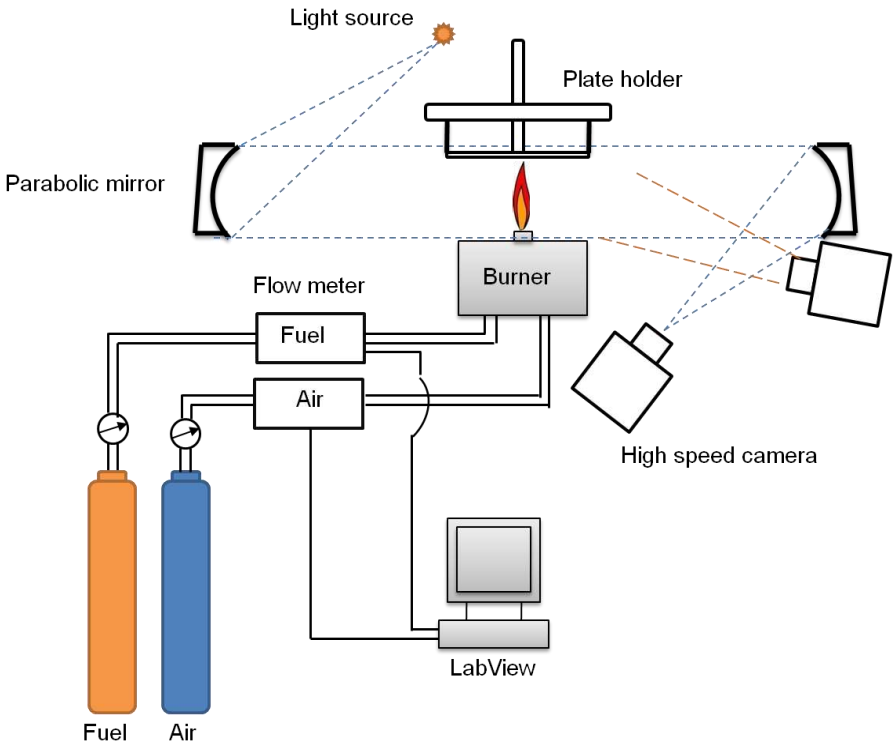

Fig.1 Schematic of the experimental setup

Table 1 Test conditions

Gas type	Volume flow rate (l/min)	Velocity (m/s)	Re No.	V_a/V_f [a]
Methane (CH_4)	0.182	0.216	55.4	/
Air	5	0.077	171	0.36
Air	14	0.216	479	1.00
Air	25	0.385	855	1.78
Air	50	0.772	1710	3.56
Air	75	1.155	2565	5.34
Air	100	1.540	3420	7.13
Air	125	1.925	4275	8.91
Air	150	2.310	5130	10.7
Air	175	2.695	5985	12.5

[a] V_a: co-flow air velocity; V_f: fuel velocity

The repeatability of the experiments was verified by measuring the hot gas movement on the schlieren images. The ignition process has been repeated for 10 times of the cases 5 l/min, 14 l/min and 50 l/min. The mean relative tolerance based on the flame propagation measurement is less than 5%, which is reasonably repeatable. Although the schlieren and direct imaging sequences were recorded separately, the good repeatability of the experiments can still enable an appropriate comparison between them. The spark initiation time can be recognised from the high speed imaging sequences.

In order to show the weak blue flame during the ignition process more clearly, DFCD method was applied to process the original colour images. By setting filters within HSV model space, the yellowish and bluish flame colourations can be identified and separated. Then the identified blue colour pixels were selectively enhanced by 35 times in the RGB model space to make the very weak blue flame observable. The comparison between the original and blue colour-enhanced images is shown in Fig. 2. It can be seen that the blue colour flame can hardly be observed on the original high speed image at a shutter speed of 1/500 s, but can be visualised clearly on the enhanced images. The results demonstrate that it can be quite misleading in interpretation of high speed or high shutter speed

flame colour images without careful digital enhancement because the blue flames are so much weaker than the yellowish flame and it can be completely masked.

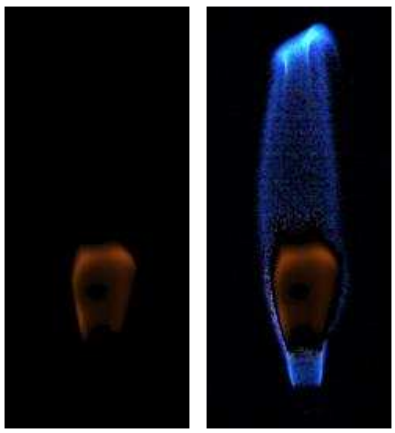

Fig.2 Comparison between the original and the blue colour-enhanced images through DFCD method (5 l/min air flow rate at 60 ms after ignition)

The velocity fields during the ignition process have been extracted from the schlieren images using optical flow method. Optical flow is considered as the distribution of the apparent velocities of movement of brightness patterns in an image [22]. The basic assumption in optical flow techniques is that the gray levels of objects in subsequent frames do not change over time. One constraint can be established based on the change in image brightness at a point on the image plane due to motion, which can be written as:

$$I_x u + I_y v + I_t = 0 \quad . \tag{1}$$

where I is the image intensity, t is the time between frames, $u = dx/dt$ and $v = dy/dt$ are velocities. In order to resolve the two unknown velocities u and v, a second constraint was composed on smoothness. It assumes that neighbouring points on the viewed object have similar velocities, while the velocity field of the image brightness patterns varies smoothly almost everywhere. In present study, the directional smoothness proposed in [23] has been applied, which considers the flow field should be smooth over the image in terms of its direction rather than its magnitude. The directional smoothness constraint equation can be written as:

$$\left(\frac{\partial(u/v)}{\partial x}\right)^2 + \left(\frac{\partial(u/v)}{\partial y}\right)^2 = 0 \quad . \tag{2}$$

Based on the two equations (1) and (2), using the optimization strategy proposed in [24], the velocity field during the ignition process has been evaluated. It is worth mentioning that only the flow field with turbulence structures have been processed for velocity estimation, which is due to the basic assumptions of optical flow method. The estimated average endpoint error (EPE) of the current optical flow technique is 0.319 pixel/frame using the Middlebury benchmark test database [24]. Considering the view field dimension and the framing rate used in current study, the flame speed error is 0.098 m/s.

3. Results and discussions

3.1 Cold flow pattern

Previous investigation indicates that the flame establishment process is closely related with the cold flow pattern before ignition. With the help of schlieren imaging, the cold flow pattern of the fuel jet before ignition can be visualised at different air coflow velocities. By examining the schlieren images, three typical cold fuel jet patterns before ignition are observed, as shown in Fig.3. When the coflow air flow rate is at 5 l/min, 14 l/min and 25 l/min, a straight and laminar fuel jet is established with the help of upward momentum of air coflow. When the air flow rate is at 50 l/min, a transient flow pattern with regular vortex shedding structure can be observed, which is mainly due to the Kelvin-Helmholtz instability. The vortex shedding frequency can be identified from the time-resolved schlieren image sequence, which is 12 Hz in this case. When the air flow rate exceeds 75 l/min, turbulent structures can be found in the cold flow pattern. The increased air speed induces strong turbulent effect, which penetrates into the core area of the fuel jet and enhances the fuel/air mixing dramatically.

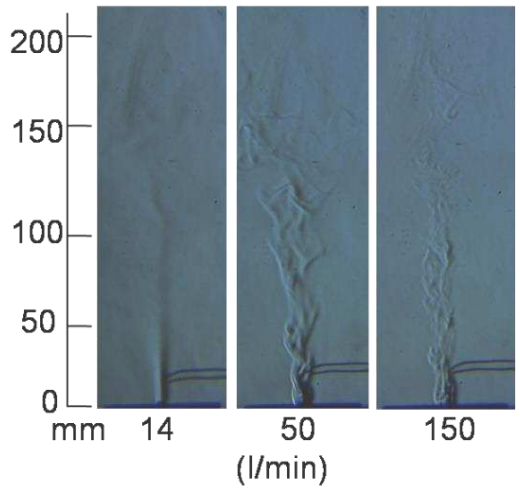

Fig. 3 Typical tested cold fuel flow patterns at different coflow air flow rates (14 l/min, 50 l/min and 150 l/min)

Mixture fraction distribution has played an important role in the ignition process. It was found from the flame images that diffusion flame can be formed when the coflow velocity is no more than 50 l/min, while premixed flame will be formed when the coflow velocity is increased further, which will be demonstrated and discussed in more details in the following sections. The main reason can be attributed to the mixture fraction variation due to the coflow air velocity. As illustrated in Fig.4a, for diffusion flame cases, the mixture fraction will vary from 0 to 1. With the increasing of coflow air velocity, the mixture fraction distribution will be steeper. For premixed flame cases, as shown in Fig.4b, the strong momentum of the coflow air will penetrate into the fuel jet center and helps to form premixed mixtures for the whole jet. The mixture fraction will change from 0 to a certain value less than 1. While the coflow air velocity increases, more air will be mixed with the fuel, which decrease the maximum value of mixture fraction. At the same time, the stronger upward momentum may make the mixture fraction distribution steeper.

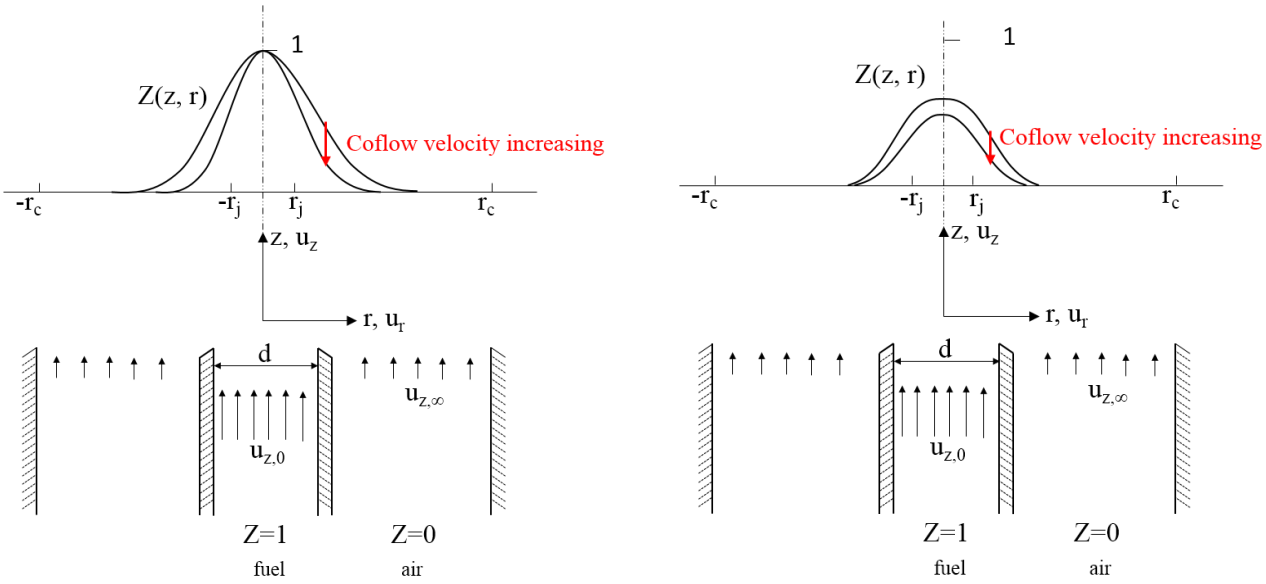

Fig. 4 Illustration of mixture fraction variation at different coflow velocities
(a) Diffusion flame for colow velocities at 5 l/min, 14 l/min, 25 l/min and 50 l/min; (b) Premixed flame for colow velocities at 75 l/min, 100 l/min, 125 l/min, 150 l/min and 175 l/min.

3.2 Diffusion flame establishment with low coflow velocities

In current study, the main focus is on the flame kernel formation and propagating characteristics under the circumstances of successful ignition cases. The overall ignition of the burner including three stages, which are (i) the formation of a flame kernel, (ii) the convection pattern in the flow and (ii) the stabilization of the flame. The ignition processes discussed in this study have experienced all these three stages.

Figures 5 and 6 show the blue colour-enhanced and schlieren image sequences of the ignition process at 5 l/min, 14 l/min, 25 l/min and 50 l/min respectively. From the comparison of schlieren and blue colour-enhanced images, it is found that the hot gas tip boundary is identical to the flame front, which indicates that the whole flame structure during the ignition can be observed completely via DFCD method. Smooth hot gas structure can be seen in the cases of 5 l/min, 14 l/min and 25 l/min, while turbulence structure is observed in the case of 50 l/min.

In the four cases shown in Figures 5 and 6, the cold flow pattern shows that the fuel jet is formed showing non-premixed characteristics, where the equivalence ratio is changing from zero to infinity from outside to the jet centre in the horizontal direction. A combustible mixture zone is formed around

the fuel jet rim due to the local fuel/air mixing. It can be seen from the colour images that, at the very beginning of the ignition, irregular blue flame kernels are formed with clear curved boundaries. Then the flame propagates along the fuel/air mixing boundaries: forming a circle in jet tangential radial direction, growing longer in jet axial direction, and the lower flame boundary attaching the nozzle exit gradually. In the four cases at low air flow rates (5 l/min, 14 l/min, 25 l/min and 50 l/min), a hollow blue flame with a brighter tip is formed at first. The blue-pocket phenomena observed in Fig.5 indicates that the flame kernel propagation will follow a route with favourable fuel/air mixing. The fuel rich mixtures begin to crack under high temperatures and a yellow-reddish flame can be observed after about 60 ms, indicating high volume concentration of soot particles. The fuel-rich flame changes colour from dark red to bright yellow, which indicates the flame temperature is increasing dramatically because of the further reaction with air. In all the four cases, a Bunsen like flame is formed near the burner nozzle. A flame necking phenomena can be observed due to the buoyancy induced Kelvin-Helmholtz instability. The flame is breaking and the upper part is moving upward like a 'hat'. In the four cases, a steady diffusion flame can be formed without oscillating finally. The flame oscillation is suppressed by the coflow air as reported in [10]. It can be observed from Fig.5 that, the steady flame occurred at 90 ms, 80 ms, 70 ms, and 80 ms for the cases of 5 l/min, 14 l/min, 25 l/min and 50 l/min respectively. The minimum time occurs for the case of 25 l/min. The main reason is that 25 l/min is a case with the maximum coflow velocity but keep laminar flow patterns for the cold flow. With the increasing of coflow velocities, the stronger upward momentum will help to make the flame steady in a shorter time. However, for the case of 50 l/min, the flow starts to show turbulence characteristics, which increase the flame unsteadiness comparing to laminar flow conditions.

In the colour images shown in Fig. 5, the red diffusion flame is observable after 60 ms, which is hard to be seen at the initial ignition stage. In order to show the red diffusion flame more clearly, the images have been processed on purpose. The flame emanating red colour is due to the continuous spectrum from solid carbon/soot, which covers the NIR and VIS spectra. The darker the flame, the longer wavelength of the emanating light. Thus the weak red flame which is hard to see in the original

image should correspond to the long wavelength in the VIS spectra and the NIR spectra. According to the spectra responding characteristics of typical colour cameras, the R value is dominate in this spectra range in the RGB model. Thus the R layer information is abstracted and displayed in grey scale, while the scale is adjusted to minimise the noise and show the red flame contour clearly. The red flame can be recognised around 30 ms after the treatment. The processed images between 32 ms and 60 ms have been shown in Fig.7. It can be seen that the starting point of yellow flame is around 32 ms for 5 l/min and 14 l/min, while around 36 ms for 25 l/min and 50 l/min. The main reason may be due to the fact that more premixed fuel/air mixtures are formed due to the enhanced fuel/air mixing with the increasing of coflow velocity, which will decrease the pure fuel portion in the flow field and also increase the time for yellow flame occurrence. It can be seen that the red flame shows hollow structure at the beginning and then propagates from outside to jet centre to form a solid contour. The red flame shape is becoming thinner and longer with the increasing of coflow air flow rates. The blue and yellow-reddish flame height changing with time has been plotted in Fig.8. It is seen that with the increasing of coflow air velocity, both the blue and yellow flame propagation speeds in upward direction are increased, mainly due to the momentum gained from coflow air.

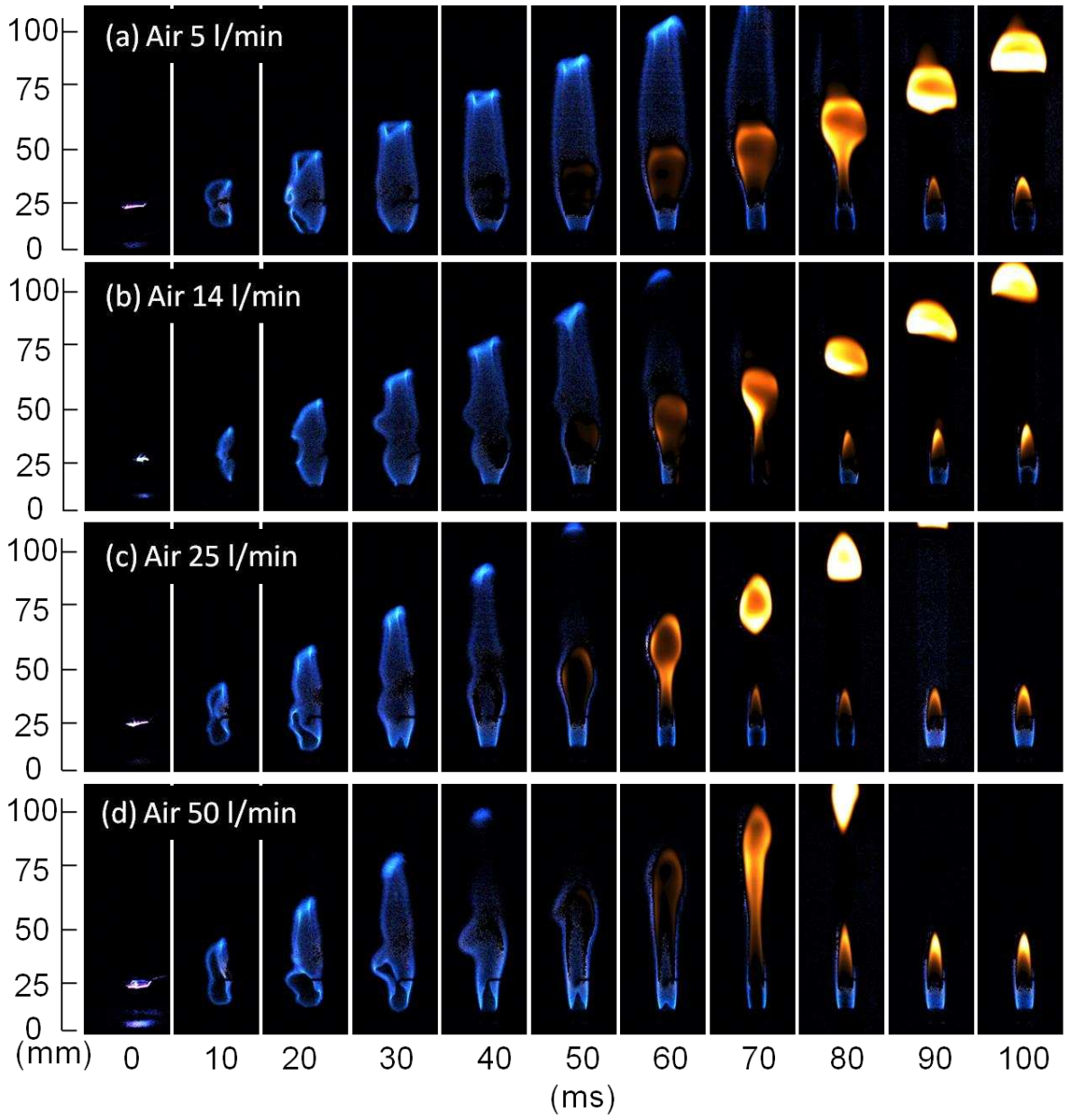

Fig. 5 Blue-colour enhanced imaging sequence at different air flow rates of (a) 5 l/min, (b) 14 l/min, (c) 25 l/min and (d) 50 l/min

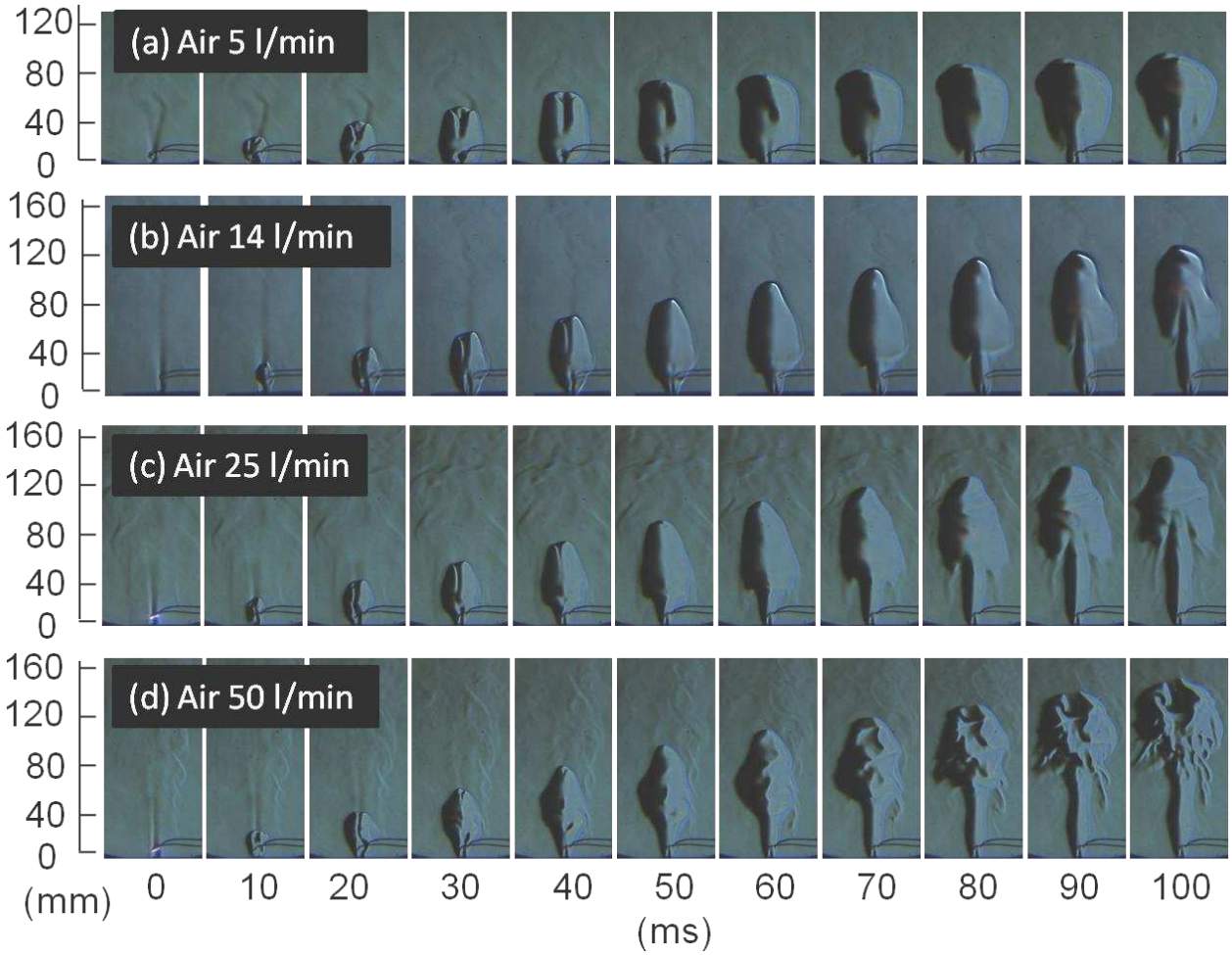

Fig. 6 Schlieren imaging sequence at different air flow rates of (a) 5 l/min, (b) 14 l/min, (c) 25 l/min and (d) 50 l/min

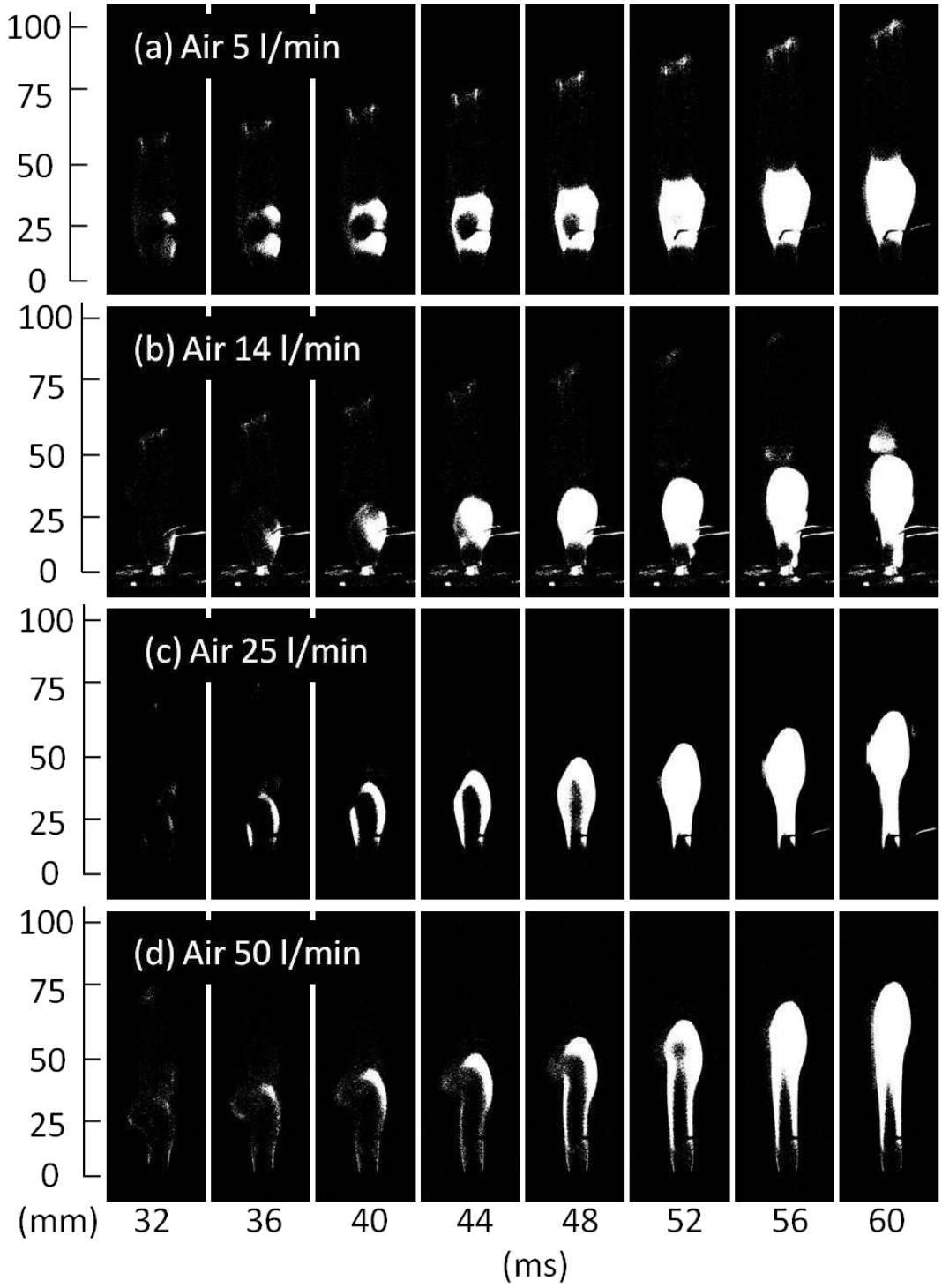

Fig. 7 Processed weak red flame contours at different air flow rates of (a) 5 l/min, (b) 14 l/min, (c) 25 l/min and (d) 50 l/min

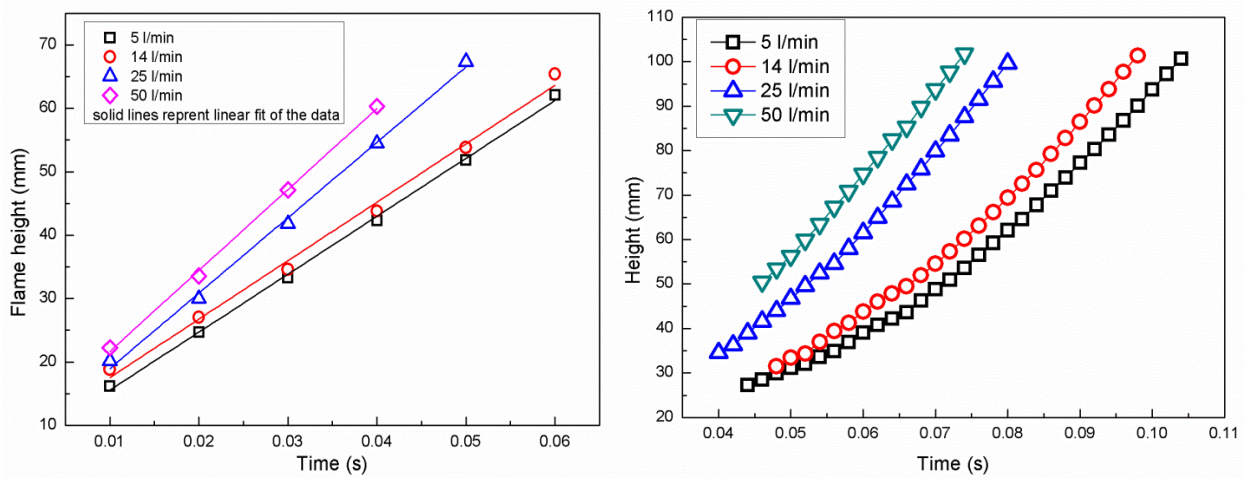

(a) (b)

Fig. 8 (a) Blue flame height at different time after ignition; (b) Yellow-reddish flame height at different time after ignition

The integration of blue and green colour intensity indicates the 1D detection of CH* and C_2* chemiluminescence emissions, which is plotted in Fig.9a-d with the variation with time. It is seen that the changing trends of blue and green colour intensities in each case are similar, while blue colour intensity is higher than green. Both blue and green intensities increase sharply after the ignition initiation, which have a peak value at 62 ms, 40 ms, 32 ms and 30 ms for the 5 l/min, 14 l/min, 25 l/min and 50 l/min respectively. After that the blue and green intensities decrease rapidly to a very low value. The variations are due to the combustion of the premixed fuel/air mixtures accumulated before ignition. The two intensities reach to a steady value after 100 ms, which is due to the blue flame occurring in the diffusion flame. The C_2*/CH* ratio of two radical chemiluminescence intensities have been previously used to provide indications of the global fuel/air mixture state of a premixed flame [16, 17], which can be estimated by the blue and green colour intensity ratio (GB ratio) at the local pixels. The characteristic mean value of the GB ratio in one image is calculated based on the Gaussian distribution algorithm. Since the GB ratio is a kind of mean value of the whole image, only the images with large blue and green intensity values from 30 ms to 60 ms have been analysed, as shown in Fig.9e. The GB ratio variation at different equivalence ratios between 0.9 and 1.5 of premixed methane flames have been obtained by Migliorini et. al [14], which shows a good match with the spectral

measurements, as shown in Fig.9f. It can be seen that most of the GB ratios in Fig.9e are in a range between 0.4 and 0.425, which indicates that the equivalence ratio is close to 1.

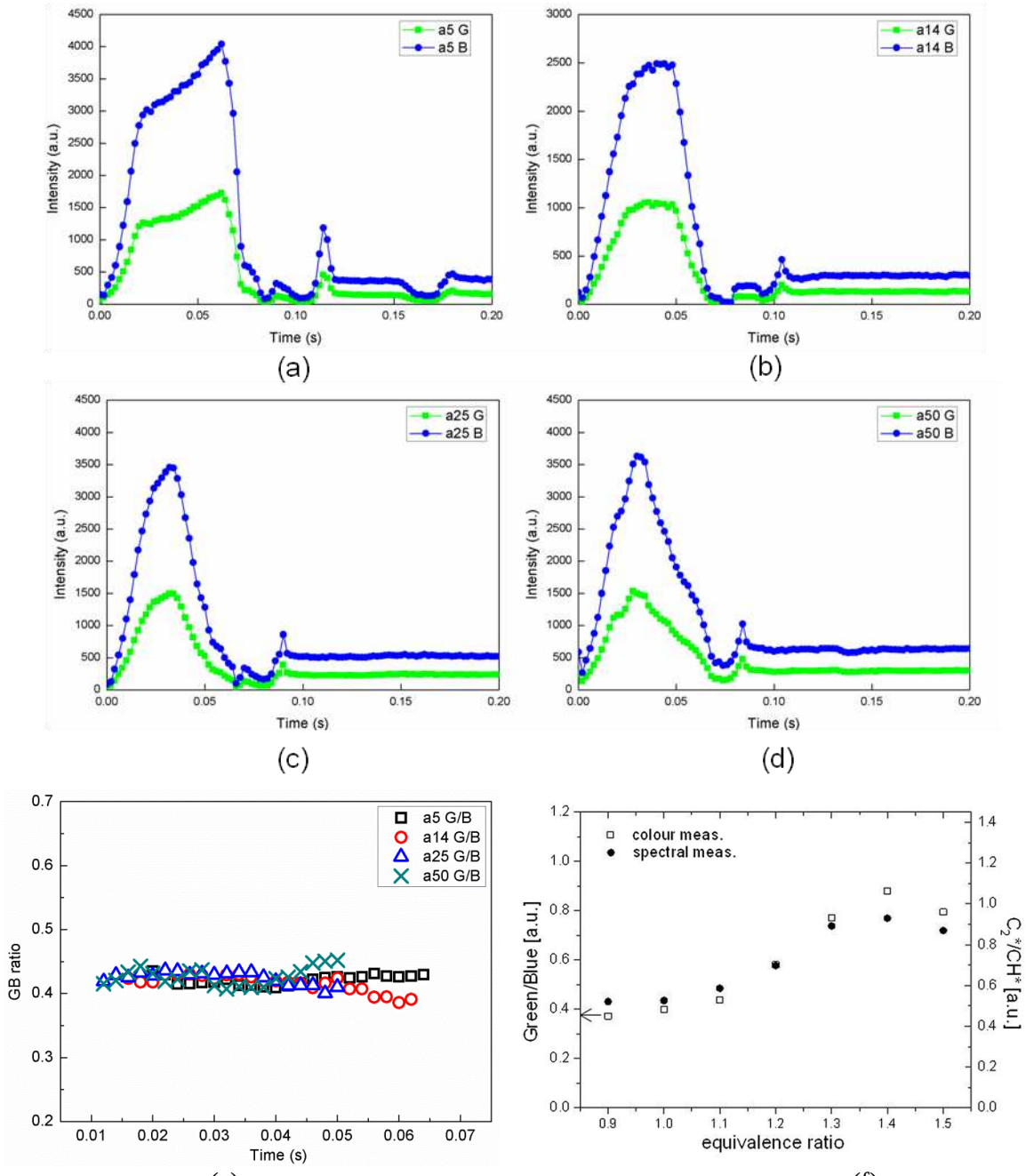

Fig. 9 (a-d) The Green and Blue intensity of blue flame variation with time; (e) The GB ratio during the ignition process; (f) The GB ratio variation at different equivalence

3.3 Premixed flame establishment with high coflow velocities

Figures 10 and 11 show the blue colour-enhanced and schlieren image sequences of the ignition process at 75 l/min, 100 l/min, 125 l/min, 150 l/min and 175 l/min respectively. When the air flow rates are higher than 75 l/min, the cold flow pattern shows turbulent structures, which indicates that

the air has penetrated into the fuel jet centre. Thus all the fuel is premixed with air before ignition. The colour images show that the flame is in blue colour only and the yellow-reddish flame is not observable any more. Two typical structures can be recognised from the schlieren images: a hot gas bulge at upper part and a laminar central jet developed from nozzle exit. The laminar pattern from the nozzle exit is due to the upward momentum effect of the coflow air. It can be seen that the tip of the top hot gas bulge and the height of the bottom laminar pattern are both increasing with time. By careful observation, it can be seen from schlieren images that the hot gas tip in Fig.11 is not as smooth as that in Fig.6, which means the strong turbulence effect destroyed the smooth flame front. Some fuel may be blown away without combustion. The quantitative velocity magnitudes of the top part of the flow field with turbulent structures have been evaluated using optical flow method, as shown in Fig. 12. It can be seen that the overall velocity is increasing with the increasing of coflow air velocities, while the maximum velocity is increasing from 1.6 m/s to 3 m/s.

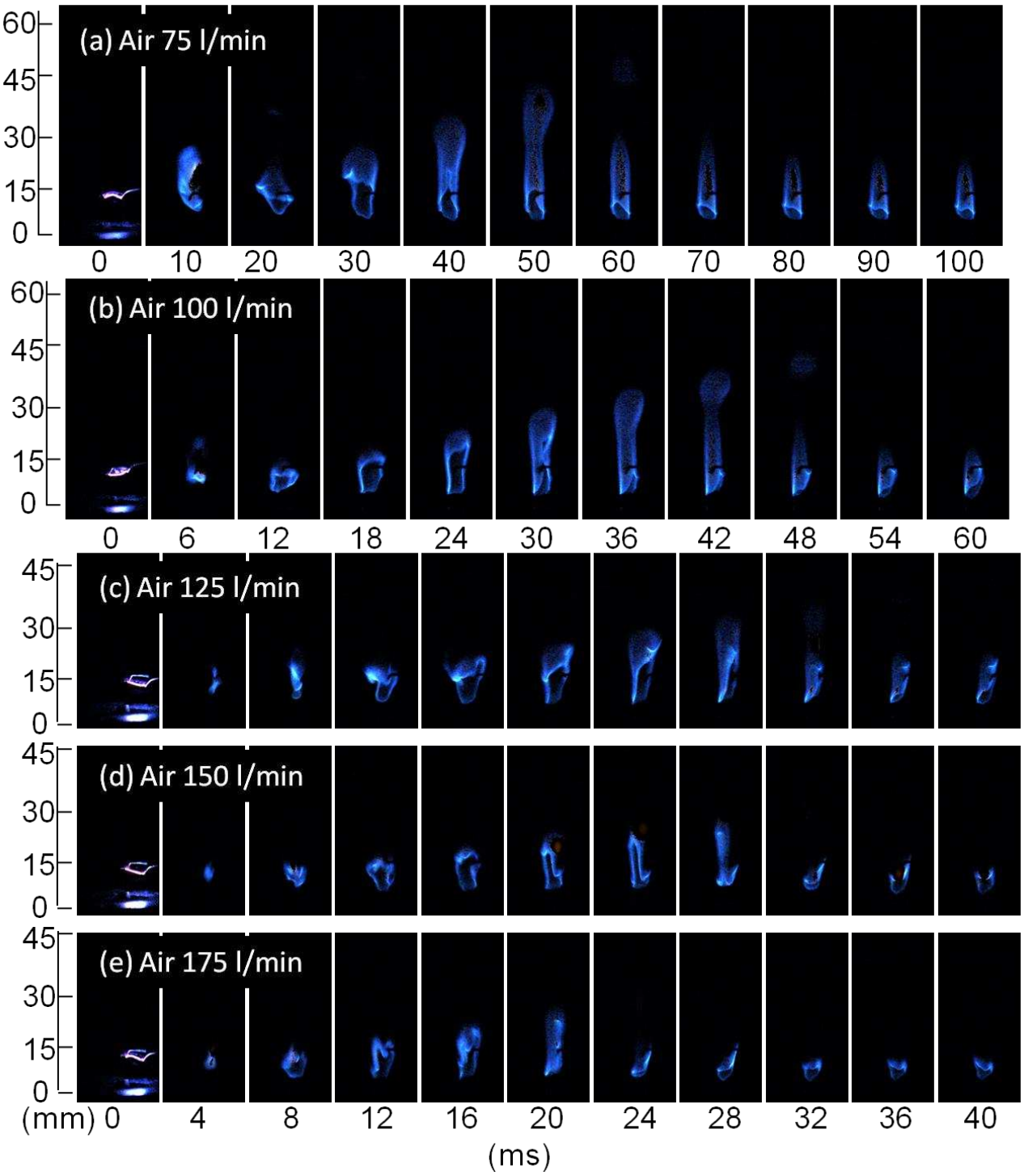

Fig. 10 Blue-colour DFCD enhanced imaging sequence at different air flow rates of (a) 75 l/min, (b) 100 l/min, (c) 125 l/min, (d) 150 l/min and (e) 175 l/min

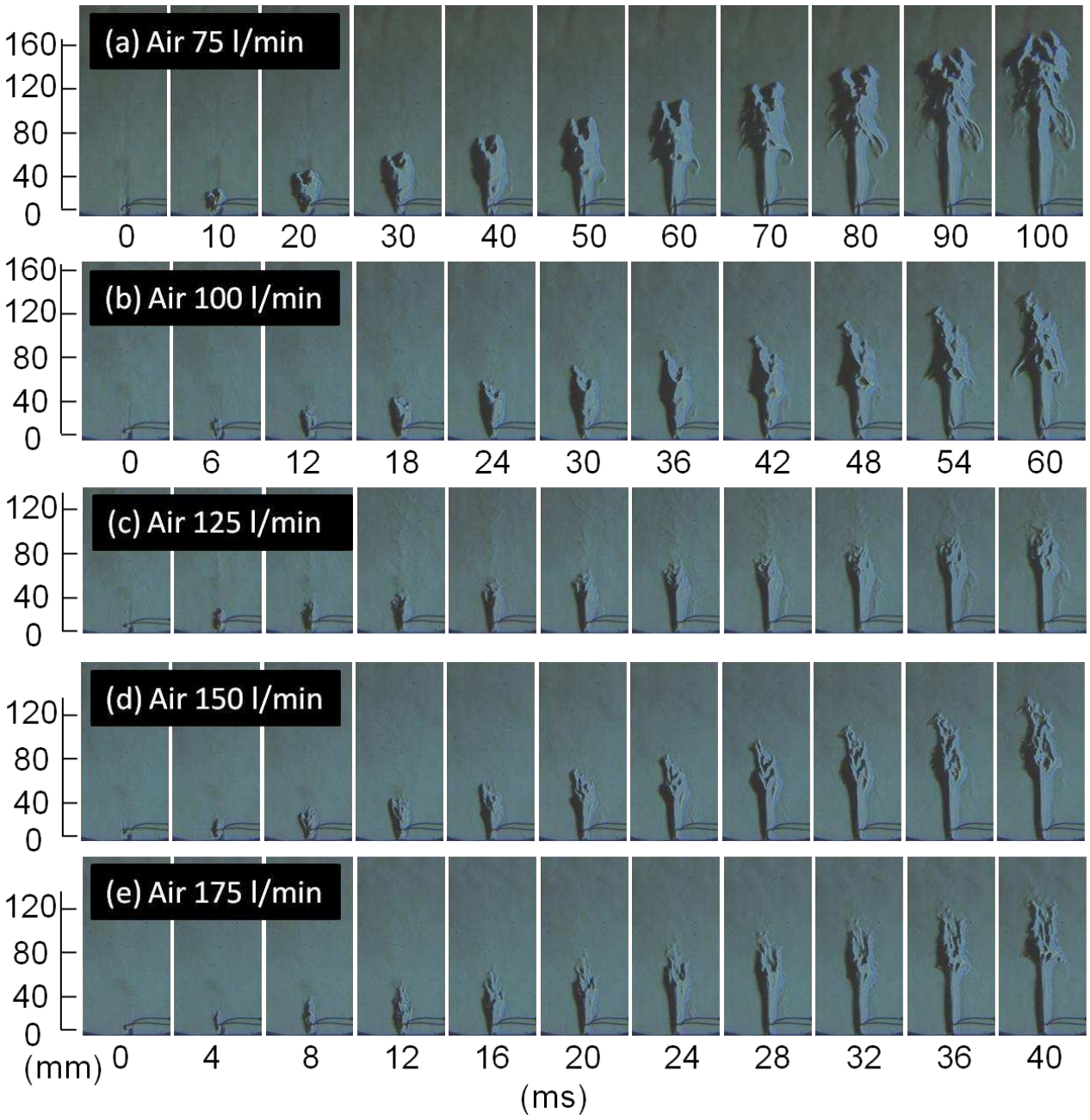

Fig. 11 Schlieren imaging sequence at different air flow rates of
(a) 75 l/min, (b) 100 l/min, (c) 125 l/min, (d) 150 l/min and (e) 175 l/min

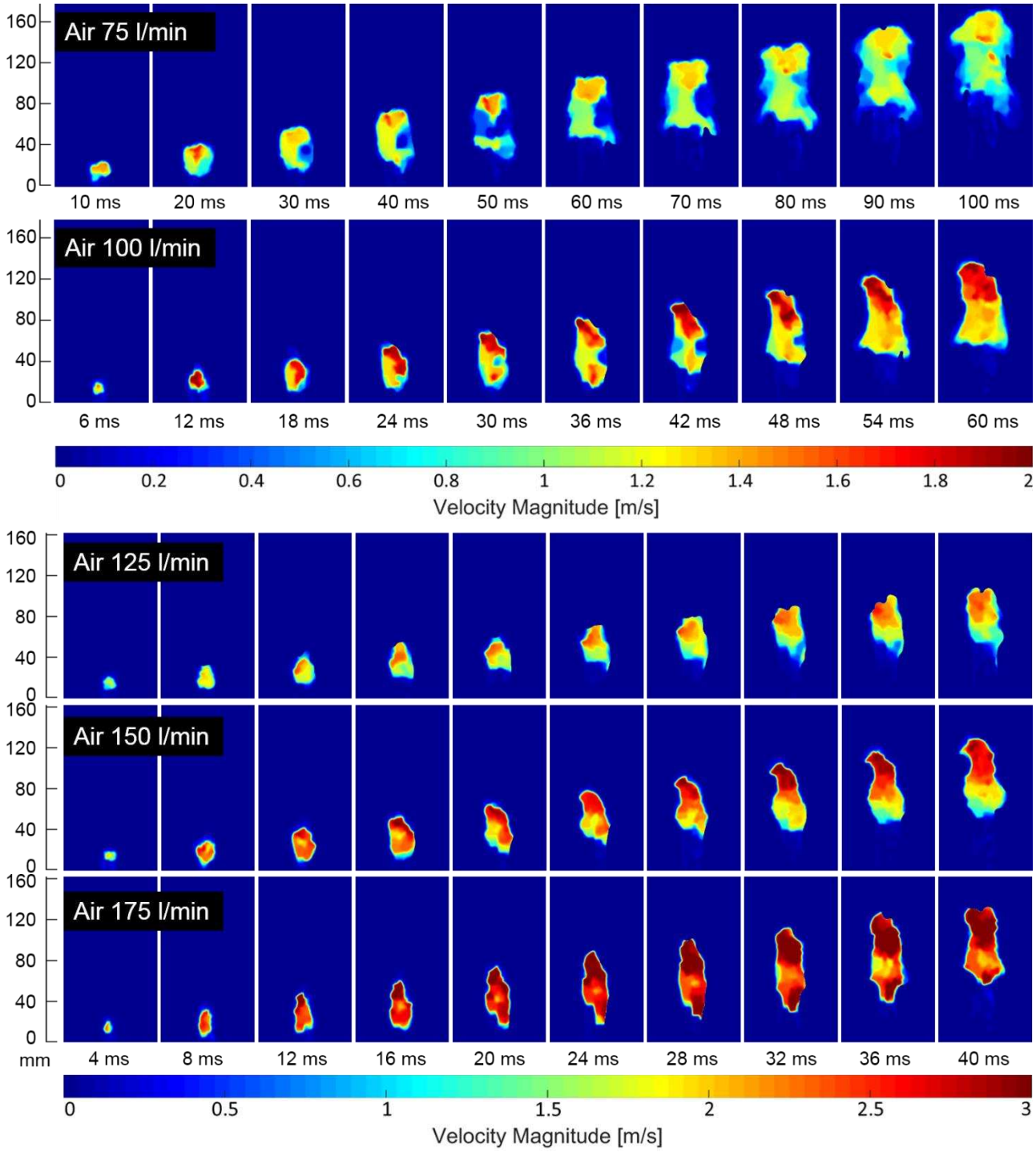

Fig. 12 Velocity fields at air flow rates of 75 l/min, 100 l/min, 125 l/min, 150 l/min and 175 l/min

In all the cases shown in Fig.10, the flames are partially lifted off the burner exit with irregular curvatures at the bottom of the flames, which is due to the strong upward momentum of the coflow air. In all the cases, the flame height is increasing with time at first as a result of the excessive fuel accumulated before ignition. The flame height starts to decay when the excessive fuel is consumed and finally reaches a steady state with a constant flame height. The flame heights at steady state is

shown in Fig.13. It can be seen that when the air flow rates exceeds 75 l/min, the steady state flame height is decreasing with the increasing coflow air velocities, because higher coflow velocity could blow more fuel away.

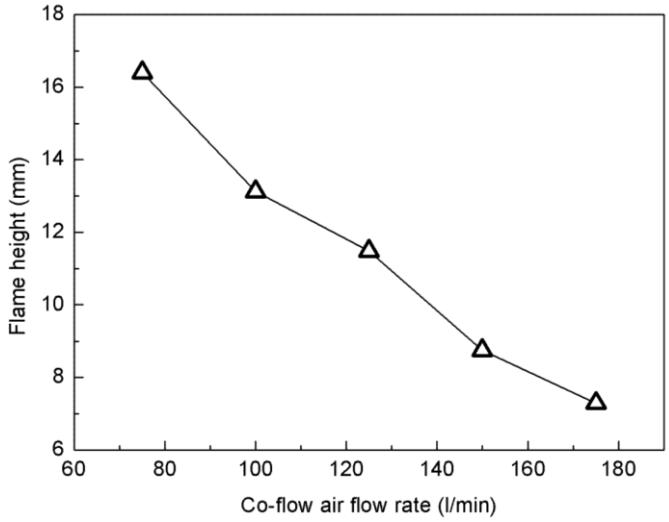

Fig.13 Flame height at steady state with different coflow air flow rates

The integration of blue and green colour intensity of the blue flame in each case has been plotted in Fig.14a-e with the variation of time. It can be seen that the changing trends of blue and green colour intensities in each case are similar, while blue colour intensity is higher than green. Both blue and green intensities increase sharply after the ignition initiation, which reach peak values at 46 ms, 32 ms, 28 ms, 26 ms and 18 ms for the 75 l/min, 100 l/min, 125 l/min, 150 l/min and 175 l/min cases respectively. After that the blue and green intensities decrease rapidly to lower values, which then keep almost constant indicating the steady stage flame establishment. The blue and green intensity variation at the very beginning is mainly due to the consumption of the accumulated fuel/air mixtures before ignition. The GB ratio has been evaluated in the five cases and plotted in Fig. 14f. It can be seen that most of the GB ratios in Fig.14e are in a range between 0.4 and 0.425, which indicates that the equivalence ratio is also close to 1.

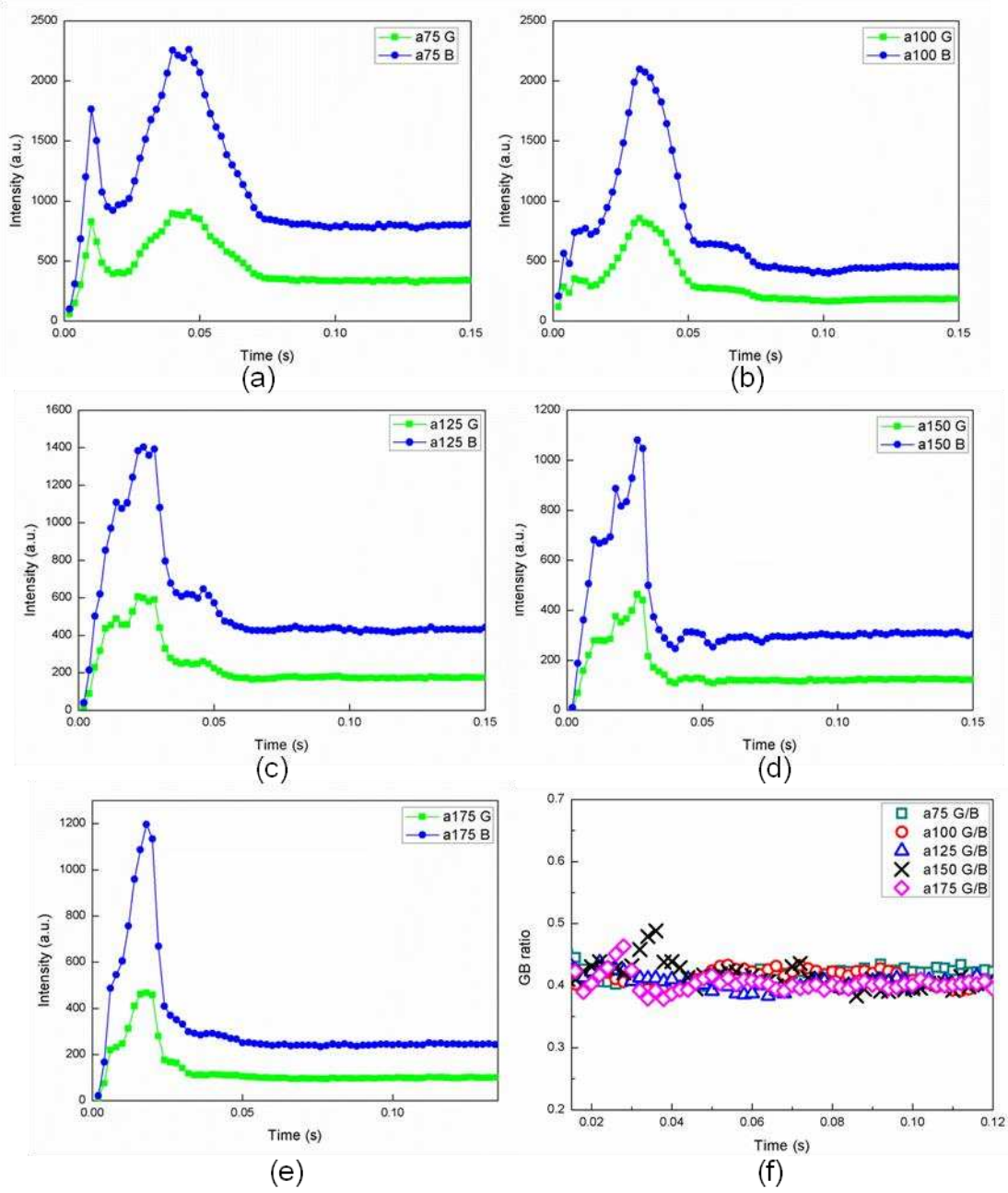

Fig. 14 (a-e) The Green and Blue intensity of blue flame variation with time; (f) The GB ratio during the ignition process.

4. Conclusions

The coflow effect on the ignition process of laminar methane diffusion flames have been investigated by visualising the DFCD enhanced weak blue flame and the invisible hot gas flow field. The burner exit velocity ratio based on the cold coflow air and fuel is tested in a wide range from 0.36 to 12.5, which corresponds to laminar flow regime at lower ratios and turbulent one at higher ratios. By enhancing the weak blue flame selectively and showing the weak yellow flame separately, the ignition process is visualized correctly. When the air flow rate is no more than 50 l/min, it is observed that the

blue flame is formed first along the fuel/air mixing region. A hollow blue-pocket is formed due to the coflow effect. The yellowish flame can be observed to form inside the blue-pocket, which indicates the fuel rich mixture is heated before initiated for chemical reactions. A typical diffusion flame can be established at low air flow rates. When the air flow rate exceeds 75 l/min, only partially lifted off blue flame is observable due to the enhanced fuel/air mixing by strong air momentum. The blue and green colour intensity of blue flame has been integrated to denote the CH* and C_2* signals. Evaluated from GB ratios, the equivalence ratio of the blue flame is close to 1 during the ignition process in all the cases. The hot gas development has been visualized based on high speed schlieren images. A laminar pattern can be observed from the nozzle exit due to the strong upward coflow air momentum coupled with combustion. The velocity fields have been estimated quantitatively using optical flow method when the flow fields have tractable turbulent structures. When the air coflow velocity is increasing from 75 l/min to 175 l/min, the flow velocity shows to increase with the coflow air velocities accordingly. The experimental investigation has revealed the flame and flow dynamics during ignition process comprehensively; the visualisation and quantitative measurement results can be served as reliable validation proof for numerical simulations.

Acknowledgements

This work is supported by the National Natural Science Foundation of China (Grant No: 51306113) and the National Natural Science Foundation of Shanghai (Grant No: 13ZR1456700) to enable the first author to conduct experiments at the University of Sheffield.

References

[1] D.S. Chamberlin, A. Rose, The flicker of luminous flames, Proc. Combust. Inst.1-2 (1948) 27-32.

[2] L.D. Chen, J.P. Seaba, W.M. Roquemore, L.P. Goss, Buoyant diffusion flames, Proc. Combust. Inst. 22 (1989) 677-684.

[3] T.Y. Toong, F.S. Richard, M.S. John, Y.A. Griffin, Mechanisms of combustion instability, Proc. Combust. Inst. 10 (1965) 1301-1313.

[4] V.R. Katta, W.M. Roquemore, Role of inner and outer structures in transitional jet diffusion flame, Combust. Flame 92 (1993) 274-282.

[5] I. Kimura, Stability of laminar-jet flames,Proc. Combust. Inst. 10 (1965) 1295-1300.

[6] J. Buckmaster, N. Peters, The infinite candle and its stability - a paradigm for flickering diffusion flames, Proc. Combust. Inst. 21 (1988) 1829–1836.

[7] S. H. Won, S.H. Chung, M.S. Cha, B.J. Lee, Lifted flame stabilization in developing and developed regions of coflow jets for highly diluted propane, Proc. Combust. Inst. 28 (2000) 2093-2099.

[8] S.H. Won, J. Kim, M.K. Shin, S.H. Chung, O. Fujita, T. Mori, J.H. Choi, K. Ito, Normal and microgravity experiment of oscillating lifted flames in coflow, Proc. Combust. Inst. 29 (2002) 37-44.

[9] B.C. Connelly, M.B. Long, M.D. Smooke, R.J. Hall, M.B. Colket, Computational and experimental investigation of the interaction of soot and NO in coflow diffusion flames, Proc. Combust. Inst. 32 (2009) 777-784.

[10] Q. Wang, H. GohariDarabkhani, L. Chen, Y. Zhang, Vortex dynamics and structures of methane/air jet diffusion flames with air coflow, Exp. Therm. Fluid Sci. 37 (2012) 84-90.

[11] E. Mastorakos, Ignition of turbulent non-premixed flames, Prog. Energy Combust. Sci. 35(2009)57-97.

[12] T.X.Phuoc, C.M.White, D.H.McNeill, Laser spark ignition of a jet diffusion flame, Opt. Laser. Eng. 38 (2002) 217-232.

[13] E.S. Richardson, E.Mastorakos, Numerical investigation of forced ignition in laminar counterflow non-premixed methane-air flames, Combust. Sci. Technol. 179 (2007) 21-37.

[14] X.Qin, C.W. Choi, A.Mukhopadhyay, I.K. Puri, S.K. Aggarwal, V.R. Katta, Triple Flame Propagation and Stabilization in a Laminar Axisymmetric Jet, Combust.Theor. Model 8 (2004) 293-314.

[15] Y. Zhang,K.N.C. Bray, The visualisation and mapping of turbulent premixed impinging flames, Combust. Flame 116 (1999) 671-674.

[16] Q. Wang, H.W. Huang, Y. Zhang, Impinging flame ignition and propagation visualisation using schlieren and colour-enhanced stereo imaging techniques, Fuel 108 (2013) 177-183.

[17] H.W.Huang, J.Yang, Q.Wang, Y.Zhang, Variation of hydrocarbon compositions and ignition locations on the radiative flame initiation characteristics through multi-dimensional dfcd incorporated image analysis, Fuel 103 (2013) 334-346.

[18] A.G.Gaydon, The Spectroscopy of Flames, Chapman and Hall, Harlow, London, 1974.

[19] H.W. Huang, Y.Zhang, Flame colour characterization in the visible and infrared spectrum using a digital camera and image processing, Meas. Sci. Technol. 19 (2008) 085406.

[20] H.W. Huang, Y. Zhang, Digital colour image processing based measurement of premixed CH4+air and C2H2+air flame chemiluminescence, Fuel 90 (2010) 48-53.

[21] H.W. Huang, Y. Zhang, Analysis of the ignition process using a digital image and colour processing technique, Meas. Sci. Technol. 22(2011) 075401.

[22] B. K. P. Horn, B. G. Schunck, Determining optical flow, J. Artificial Intelligence Res. 17, 185-203 (1981).

[23] S. Fu, Y. Wu, Detection of velocity distribution of a flow field using sequences of schlieren images, Opt. Eng. 40(2001)1661-1666.

[24] Sun D, Roth S, Black MJ. Secrets of optical flow estimation and their principles. IEEE CVPR, 2010. DOI: 10.1109/CVPR.2010.5539939.